Long-term Retinal Function and Structure Rescue Using Capsid Mutant AAV8 Vector in the *rd10* Mouse, a Model of Recessive Retinitis Pigmentosa

Ji-jing Pang[1,2], Xufeng Dai[1,2], Shannon E Boye[2], Ilaria Barone[3], Sanford L Boye[2], Song Mao[2], Drew Everhart[4], Astra Dinculescu[2], Li Liu[2], Yumiko Umino[4], Bo Lei[5], Bo Chang[6], Robert Barlow[4,*], Enrica Strettoi[3] and William W Hauswirth[2]

*[1]Eye Hospital, School of Ophthalmology & Optometry, Wenzhou Medical College, Wenzhou, Zhejiang, China; [2]Department of Ophthalmology, University of Florida, Gainesville, Florida, USA; [3]CNR Neuroscience Institute, Pisa, Tuscany, Italy; [4]The Center for Vision Research, State University of New York Upstate Medical University, Syracuse, New York, USA; [5]Ophthalmology, the First Affiliated Hospital of Chongqing Medical University, Chongqing Key Laboratory of Ophthalmology, Chongqing, China; [6]The Jackson Laboratory, Bar Harbor, Maine, USA. *Deceased*

The retinal degeneration 10 (*rd10*) mouse is a well-characterized model of autosomal recessive retinitis pigmentosa (RP), which carries a spontaneous mutation in the β subunit of rod cGMP-phosphodiesterase (PDEβ). *Rd10* mouse exhibits photoreceptor dysfunction and rapid rod photoreceptor degeneration followed by cone degeneration and remodeling of the inner retina. Here, we evaluate whether gene replacement using the fast-acting tyrosine-capsid mutant AAV8 (Y733F) can provide long-term therapy in this model. AAV8 (Y733F)-smCBA-PDEβ was subretinally delivered to postnatal day 14 (P14) *rd10* mice in one eye only. Six months after injection, spectral domain optical coherence tomography (SD-OCT), electroretinogram (ERG), optomotor behavior tests, and immunohistochemistry showed that AAV8 (Y733F)-mediated PDEβ expression restored retinal function and visual behavior and preserved retinal structure in treated *rd10* eyes for at least 6 months. This is the first demonstration of long-term phenotypic rescue by gene therapy in an animal model of PDEβ-RP. It is also the first example of tyrosine-capsid mutant AAV8 (Y733F)-mediated correction of a retinal phenotype. These results lay the groundwork for the development of PDEβ-RP gene therapy trial and suggest that tyrosine-capsid mutant AAV vectors may be effective for treating other rapidly degenerating models of retinal degeneration.

Received 23 August 2010; accepted 10 November 2010; published online 7 December 2010. doi:10.1038/mt.2010.273

INTRODUCTION

Retinitis pigmentosa (RP) is a family of inherited diseases causing retinal degeneration and eventual photoreceptor cell death. Visual loss in RP patients is progressive, with rod photoreceptor degeneration typically preceding cone photoreceptor loss. There is currently no treatment for this debilitating disorder. A common form of autosomal recessive RP has been linked to mutations in the β-subunit of rod cGMP-phosphodiesterase (PDEβ), which is encoded by the *Pde6b* gene.[1] cGMP-PDE controls the levels of cGMP and Ca^{2+} in rod outer segments. Improper function of cGMP-PDE causes an accumulation of cGMP within photoreceptors and prevents these cells from processing input light efficiently. Accounting for ~5% of all cases, *Pde6b*-RP is one of the earliest onset and most aggressive forms of this disease.[1–3]

Therapeutic approaches have been tested in two mouse models of RP carrying different mutations in *Pde6b*, the *rd1* and retinal degeneration 10 (*rd10)* mice. Progress in developing a therapy has been hampered by the very rapid retinal degeneration seen in the *rd1* model that initiates at or before photoreceptor outer segments even form.[4–6] Natural history studies suggest that the *rd10* mouse, which carries a point mutation in exon 13 of *Pde6b*, better emulates the progression of typical human autosomal recessive RP than the previously described *rd1* mouse.[7–9] Loss of photoreceptors in the *rd10* mouse begins around P18, with peak photoreceptor death occurring at P25.[9] Most photoreceptor cells are lost by 5 weeks.[7–9] Similar to that seen in the *rd1* mouse,[10,11] this cell death in *rd10* is accompanied and followed by structural and functional changes in the inner retina.[9] Such remodeling has also been documented in RP patients.[12] Remodeling occurs primarily in bipolar and horizontal cells by progressive dendritic retraction and loss of synaptic connections as photoreceptors initiate cell death, and is followed by glial and amacrine cell remodeling[9–11,13–21] with ganglion cell sparing.[22–24] In addition, some neuronal processes become hypertrophic and sprout ectopically. Ultimately, bipolar and horizontal cells are also lost. Interestingly, when photoreceptor death coincides with outer retinal synaptogenesis, dendrites do not develop properly, suggesting a possible trophic dependence of second order neurons on the presence of photoreceptors for maintenance of their proper morphology.[10] Thus, gene therapy-mediated preservation of photoreceptors, even relatively

The first two authors contributed equally for this work.

Correspondence: *Ji-jing Pang, Eye Hospital, School of Ophthalmology & Optometry, Wenzhou Medical College, Wenzhou, China 325027. E-mail: jpang@ufl.edu*

late in the course of degeneration may have a positive effect on inner retinal remodeling. Notably, photoreceptor cell loss occurs after terminal differentiation of the *rd10* retina. Thus, the rate of photoreceptor loss in the *rd10* mouse is substantially delayed and slower than that seen in the *rd1* retina. Rearing *rd10* mice in darkness further slows the rate of retinal degeneration by as much as 4 weeks.[8,25] Taken together, these studies suggest the *rd10* mouse is a better model in which to test RP therapeutic strategies. Various approaches for preserving retinal structure and function in *rd10* mice have been used including stem cell, antiapoptotic, antioxidant and gene-replacement therapies,[25–27] all of which have shown only a partial and/or short-term measure of retinal rescue.

We have previously shown that serotype 5, adeno-associated virus (AAV) vector containing a minimal chicken β actin promoter/CMV enhancer (smCBA) was capable of delivering functional PDEβ to the *rd10* retina.[25] Following P14 treatment with this photoreceptor-preferential AAV serotype, we showed that rod and cone-mediated function and structure were preserved for at least 3 weeks.[25] However, by 6 weeks post-treatment, therapeutic effects had faded. Because AAV5-mediated transgene expression occurs 1–2 weeks after injection in the retina[25] and photoreceptor apoptosis initiates around P16–P18 in the *rd10* mouse, it is possible that P14 treatment with standard AAV5 did not elicit sufficient PDEβ expression early enough in the *rd10* retina to arrest the degenerative progression, and therefore was insufficient to provide long-lasting therapeutic benefit.

Recent studies showed that the photoreceptor-preferential serotype 8 AAV (AAV8) vector was effective at restoring retinal structure and function to animal models of retinal degeneration which were previously shown to be refractory to AAV2 or AAV5 treatment.[28,29] Investigators attributed this to the more rapid onset of transgene expression mediated by AAV8 relative to other serotypes.[30] In addition, recent reports demonstrate that phosphorylation of tyrosine residues in AAV capsid proteins greatly affect the transduction characteristics of this vector system.[31,32] It has been shown that inhibiting phosphorylation results in strengthening of transgene expression levels and an increase in transduction kinetics relative to standard AAV.[33] The proposed mechanism is that reduced phosphorylation of surface tyrosine residues decreases ubiquitination and proteosome-mediated degradation, thereby facilitating nuclear transport of AAV vector.[31] Subsequent to this finding, AAV2 vectors with surface tyrosine residues mutated to phenylalanine (Y to F) were shown to have increased transduction characteristics relative to unmodified capsid *in vitro* and in murine hepatocytes.[32] Bearing these results in mind, we have previously shown that serotype 8 AAV containing a single point mutation (Y733F) in a surface-exposed tyrosine residue confers earlier onset and stronger transgene expression in photoreceptor cells than standard AAV8.[33] Here we report that strong and fast-acting AAV8-733 vector mediating PDEβ expression is capable of preserving retinal structure and function in the *rd10* retina for the long term. This is the first demonstration of long-term restoration of vision by gene therapy in an animal model of *Pde6b*-RP. In addition, this is the first demonstration that an AAV8 tyrosine-capsid mutant is capable of conferring more effective therapy than that of a standard AAV vector in an animal model of retinal disease. These results lay the groundwork for the development of an AAV-based gene therapy vector for treatment of patients with the *Pde6b* form of RP and support the use of AAV tyrosine-capsid mutants for the treatment of other rapidly degenerating models of retinal degeneration.

RESULTS

Optomotor behavior reveals the efficacy of AAV8 (Y733F)-smCBA-PDE β for rescue of both photopic and scotopic vision in treated *rd10* eyes

Optomotor behavioral analysis showed that uninjected wild-type eyes (**Figure 1**, black bars, $n = 4$) responded significantly better than untreated *rd10* eyes (black bars, $n = 4$, $P < 0.05$), but similar to treated *rd10* eyes (gray bars, $n = 4$, $P > 0.05$) under all conditions. Under dark-adapted conditions (**Figure 1**, top), treated *rd10* eyes had an acuity of 0.493 ± 0.089 cycles/degree (cyc/deg) (white bar, $n = 4$), a level essentially identical to that of wild-type eyes (0.499 ± 0.039 cyc/deg, black bar, $n = 4$) and significantly better than that of untreated *rd10* eyes (gray bar, 0.098 ± 0.087, $n = 4$, $P < 0.001$). Dark-adapted contrast sensitivities (**Figure 1**) were similar to scotopic acuity results; treated *rd10* eyes (contrast sensitivity of 6.338 ± 4.246, $n = 4$) showed contrast thresholds similar to uninjected wild-type eyes (4.398 ± 0.739, $n = 4$, $P = 0.425$), but performed significantly better than untreated *rd10* eyes, which displayed a contrast sensitivity of 1.05 ± 0.03 ($n = 4$, $P < 0.05$). In all scotopic tests, untreated *rd10* eyes performed extremely poorly, essentially equivalent to a lack of rod-mediated visual function. Under photopic, cone-dominated conditions, wild-type eyes showed an average acuity of 0.499 ± 0.39 cyc/deg (**Figure 1**, black bar, $n = 4$) and an average contrast sensitivity of 8.793 ± 2.790 (**Figure 1**, black bar, $n = 4$). Treated *rd10* eyes exhibited improved acuity (0.493 ± 0.089 cyc/deg, $n = 4$, $P < 0.001$) and contrast sensitivity (20.405 ± 7.196, $n = 4$, $P < 0.001$) relative to untreated *rd10* eyes (acuity = 0.098 ± 0.087 cyc/deg and contrast sensitivity= 1.075 ± 0.053, $n = 4$ each). Statistical comparisons of all behavioral measurements are shown in **Table 1**.

AAV tyrosine-capsid mutant vector AAV8 (Y733F) restores retinal function (ERG) to the *rd10* mouse in the long term whereas standard AAV5 and AAV8 vectors do not

Six months following treatment with AAV8 (Y733F)-smCBA-PDEβ, *rd10* mice were examined by dark- and light-adapted electroretinograms (ERGs). Most of the dark-adapted (**Figure 2a**) and the majority of the light-adapted (**Figure 2b**) ERG signal amplitudes were maintained in treated *rd10* eyes. In contrast, ERG signals under both conditions were almost undetectable in untreated *rd10* eyes. Rescue was most evident in eyes that experienced the largest retinal detachment during vector administration and the least surgical complications (data not shown). Restored scotopic ERGs exhibited typical a-wave structure and the average b-wave amplitudes at 0.4 log cd-s/m^2 intensity were 501.67 ± 21.19 ($n = 3$), 289.87 ± 26.24 ($n = 3$), and 12.57 ± 4.20 ($n = 3$) in normal uninjected C57BL/6J, treated and untreated *rd10* eyes, respectively (**Figure 2c**). Photopic ERG amplitudes at 1.4 log cd-s/m^2 intensity were 106.67 ± 7.12 ($n = 3$), 81.37 ± 7.12 ($n = 3$) and 8.13 ± 4.74 ($n = 3$) in normal C57BL/6J, treated and untreated *rd10* eyes, respectively (**Figure 2d**). Dark-and light-adapted b-wave amplitudes in treated *rd10* eyes were ~58%

and 68% of those from age-matched, uninjected C57BL/6J eyes. A paired *t*-test analysis revealed a significant difference between b-wave amplitudes of AAV8(Y733F)-smCBA-PDEβ-treated and untreated *rd10* eyes under both dark- and light-adapted conditions ($P < 0.01$) although a statistical difference was also found between normal uninjected C57BL/6J and treated *rd10* eyes ($P < 0.05$). To test the sensitivity of the rod and cone system in treated eyes, we measured the implicit time of the rod- and cone-driven b-waves. We found no significant difference in implicit times of the rod-driven b-waves between the treated *rd10* eyes (74.33 ± 4.04 ms) and C57BL/6J eyes (72.33 ± 2.08 ms, $n = 3$, $P = 0.597$). Likewise, no significant difference was found in implicit times of the cone-driven b-waves between the treated *rd10* (56.67 ± 5.77 ms) and C57BL/6J eyes (53.33 ± 5.77 ms, $n = 3$, $P = 0.423$).

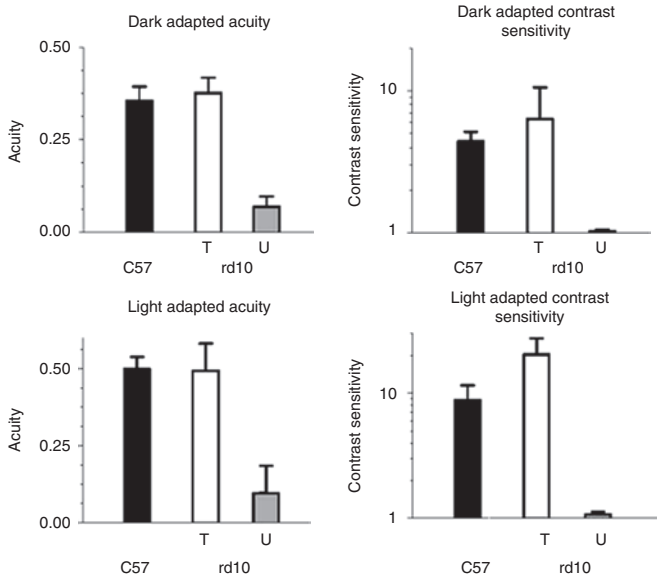

Figure 1 AAV8 (Y733F)-smCBA-PDEβ treatment at P14 restores both scotopic and photopic visual acuity and contrast sensitivity in *rd10* eyes. Under dark-adapted (top) or light-adapted (bottom) conditions, the visual acuity (left) and contrast sensitivity (right) in treated (T) *rd10* eyes (T, $n = 4$) are similar to those of wild-type animals (C57). Untreated (U) *rd10* eyes (U, $n = 4$) show very poor acuity and contrast sensitivity under either dark- or light-adapted conditions.

To highlight the effectiveness of AAV8 (Y733F)-mediated treatment relative to standard photoreceptor-selective serotypes, AAV5 and AAV8, we compared rod and cone-mediated ERG amplitudes in mice injected at P14 with different vectors at 4 weeks, 8 weeks, and 6 months after treatment (**Figure 3**). At 4 weeks after treatment, rod and cone-mediated ERG responses were highest in *rd10* mice treated with AAV8 (Y733F)-smCBA-PDEβ (**Figure 3**, left). This mutant serotype elicited even higher response amplitudes over the next 4 weeks as indicated in the 8 weeks after measurements (**Figure 3**, middle). At 8 weeks after treatment, rod and

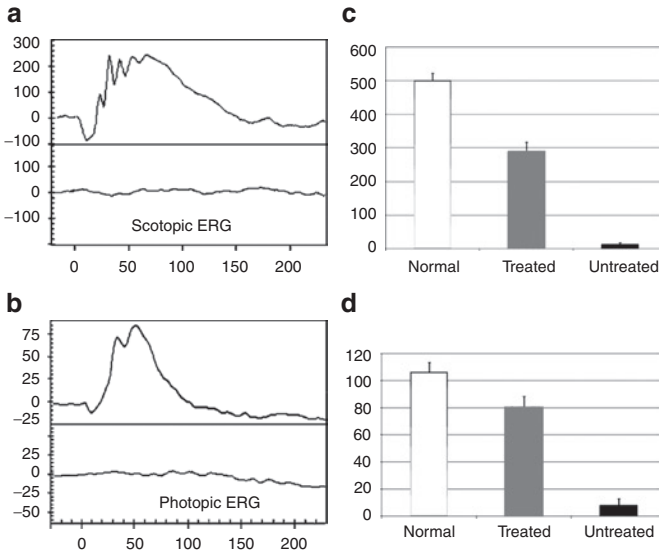

Figure 2 Scotopic and photopic electroretinogram (ERG) in treated and untreated *rd10* eyes. (**a**) Representative scotopic ERG elicited from 0.4 log cd-s/m² intensity in an *rd10* eye 6 months following treatment at P14 (upper) compared with that of the untreated eye (lower) from the same *rd10* mouse; y axis: 20 µV/Div, x axis: 50 ms/Div. (**b**) Representative photopic ERGs elicited at 1.4 log cd-s/m² from the same *rd10* mouse (upper, treated; lower, untreated); y axis: 5 µV/Div, x axis: 10 ms/Div. (**c**) Average scotopic b-wave amplitudes elicited at 0.4 log cd-s/m² in age-matched, uninjected normal C57 BL/6J (left), treated (middle), and untreated (right) *rd10* eyes; (**d**) Averaged photopic b-wave amplitudes elicited at 1.4 log cd-s/m² in age-matched, uninjected normal C57 BL/6J (left), treated (middle), and untreated (right) *rd10* eyes.

Table 1 Statistical comparison of the scotopic and photopic visual function of wild type, P14 vector-treated and untreated *rd10* mouse eyes as measured by optomotor behavior

Dark-adapted acuity ($n = 4$)			Dark-adapted contrast sensitivity ($n = 4$)		
C57BL/6J	**Treated rd10**	**Untreated rd10**	**C57BL/6J**	**Treated rd10**	**Untreated rd10**
0.355 ± 0.039	0.377 ± 0.042	0.069 ± 0.028	4.398 ± 0.739	6.338 ± 4.246	1.028 ± 0.025
C57BL/6J versus treated rd10: $P = 0.5306$	Treated versus untreated rd10: $P = 0.0002$***		C57BL/6J versus treated rd10: $P = 0.425$	Treated versus untreated rd10: $P = 0.044$*	
Light-adapted acuity ($n = 4$)			**Light-adapted contrast sensitivity ($n = 4$)**		
C57BL/6J	**Treated rd10**	**Untreated rd10**	**C57BL/6J**	**Treated rd10**	**Untreated rd10**
0.499 ± 0.039	0.493 ± 0.089	0.098 ± 0.087	8.793 ± 2.790	20.405 ± 7.196	1.075 ± 0.053
C57BL/6J versus treated rd10: $P = 0.9230$	Treated versus untreated rd10: $P = 0.0008$ ***		C57BL/6J versus treated rd10: $P = 0.097$	Treated versus untreated rd10: $P = 0.0006$***	

Under scotopic and photopic conditions, AAV8 (Y733F)-smCBA-PDEβ treatment of *rd10* eyes produces visual acuity and contrast sensitivity similar to wild-type animals. Each mouse was tested for four to six trials per condition. Data from each cohort of animals ($n = 4$) were then averaged to obtain the means for each test condition. The standard deviation listed is the standard deviation of the individual mouse means (mean ± SD). *P* values were calculated using a paired two-tailed *t*-test. ***$P < 0.001$, *$P < 0.05$.

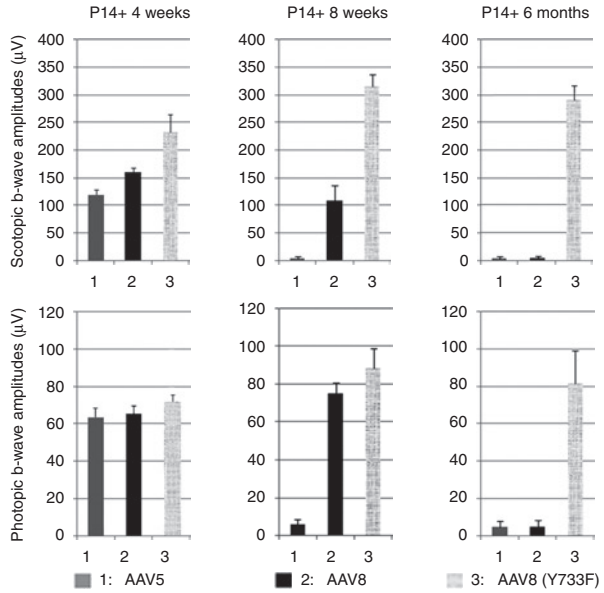

Figure 3 Comparisons of retinal function in adeno-associated virus vectors of serotype 5 (AAV5), AAV8, and AAV8 (Y733F)-treated *rd10* mice over time. (1) AAV5, (2) AAV8, (3) AAV8 (Y733F)-mediated gene therapy all have rescue effects 4 weeks after P14 treatment both in scotopic (upper, left) and photopic (lower, left) conditions. AAV8 and AAV8 (Y733F) both have rescue effects 8 weeks following injections (middle column). Only AAV8 (Y733F) has rescue effect 6 months following P14 treatment both in scotopic (upper, right) and photopic (lower, right) conditions.

cone-mediated function was undetectable in AAV5-treated *rd10* mice, whereas AAV8-treated *rd10* mice still displayed measurable rod-mediated function and robust cone-mediated function (**Figure 3**, middle). By 6 months after treatment, rod and cone responses were undetectable in AAV8-treated *rd10* mice (**Figure 3**, right). AAV8 (Y733F) was the only vector which elicited rod and cone-mediated ERG responses at 6 months after treatment indicating that this serotype is superior to standard AAV5 and AAV8 vectors in its ability to restore long-term and stable function to photoreceptors in the *rd10* mouse. Similar results were also obtained from those *rd10* mice raised in normal 12 hours/12 hours vivarium cycling room light (**Supplementary Figure S1**).

AAV8 (Y733F)-smCBA-PDEβ preserves retinal structure in treated *rd10* eyes

Spectral domain optical coherence tomography (SD-OCT) allows retinal thickness assessment in treated versus untreated eyes, *in vivo*. OCT examination revealed that AAV8 (Y733F)-mediated PDEβ expression is capable of preserving retinal morphology in treated *rd10* retinas. In order to compare the retinal thickness of treated and untreated retinas of the same mouse in an unbiased manner, a representative *rd10* mouse that displayed >90% retinal detachment in its treated eye (considered a very good subretinal injection) was carefully measured in eight comparable retinal areas, 3 mm from the optic nerve (ON) head in both treated and untreated eyes. Comparisons of retinal thickness revealed that the thickness of untreated *rd10* retina was 0.108 ± 0.007 mm ($n = 8$), while it was 0.138 ± 0.011 mm ($n = 8$, $P < 0.001$) in treated *rd10* retina. This difference in retinal thickness is clearly visible

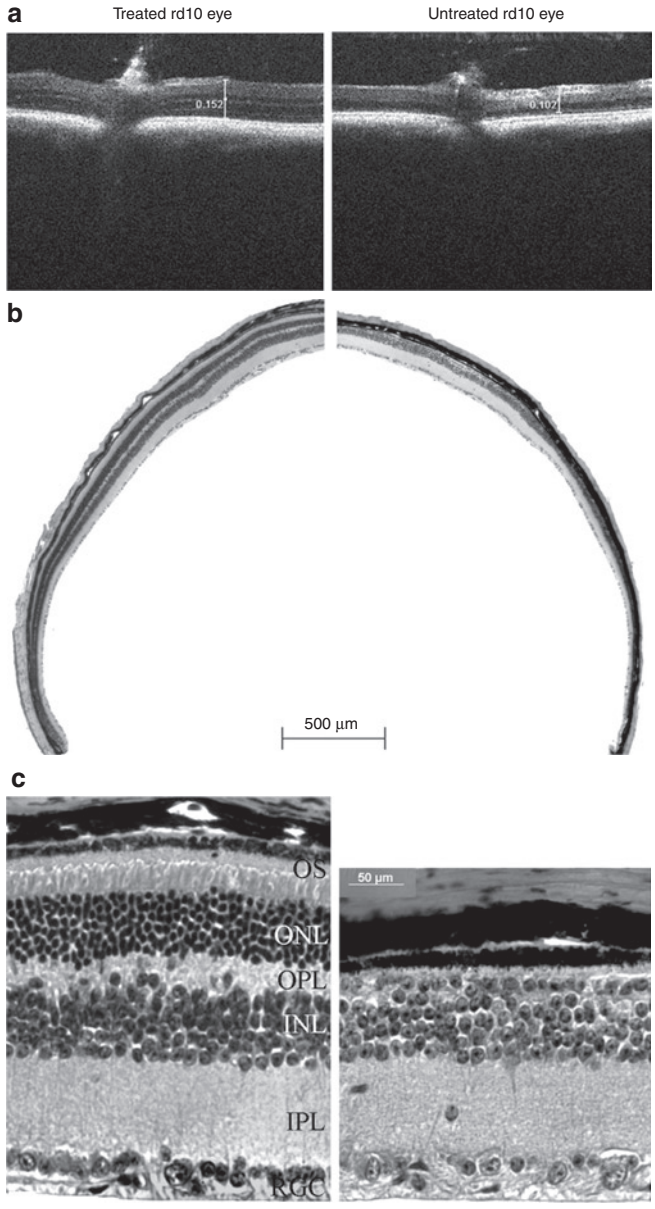

Figure 4 Bioptigen spectral domain optical coherence tomography (SD-OCT) and light microscopic (LM) images of treated (left) and untreated (right) eyes from one *rd10* mouse. (**a**) OCT images at same location (3 mm temporal to the optic nerve) from representative treated and untreated *rd10* eyes. Scale calipers on each image are placed at equivalent distances from the optic nerve to quantify the distance from the vitreal face of the ganglion cell layer to the apical face of the RPE (152 millimeters for the treated eye and 102 millimeters for the untreated eye). (**b**) Low-magnification images from the treated and untreated eyes of the same *rd10* mouse used in **a**. Note the presence of outer segments and continuous, intact outer nuclear layer (ONL) in the treated eye and their absence in the untreated eye. (**c**) High magnification LM images from the treated and untreated eyes of the same *rd 10* mouse used in **b**. OS, outer segments; OPL, outer plexiform layer; INL, inner nuclear layer; IPL, inner pexiform layer; RGC, retinal ganglion cell.

in a representative image taken 3 mm temporal of the ON head (**Figure 4a**).

Studies have shown that OCT measurements of retinal thickness correspond to follow-up histological measurements.[34] Indeed, following killing and enucleation at 6 months after treatment,

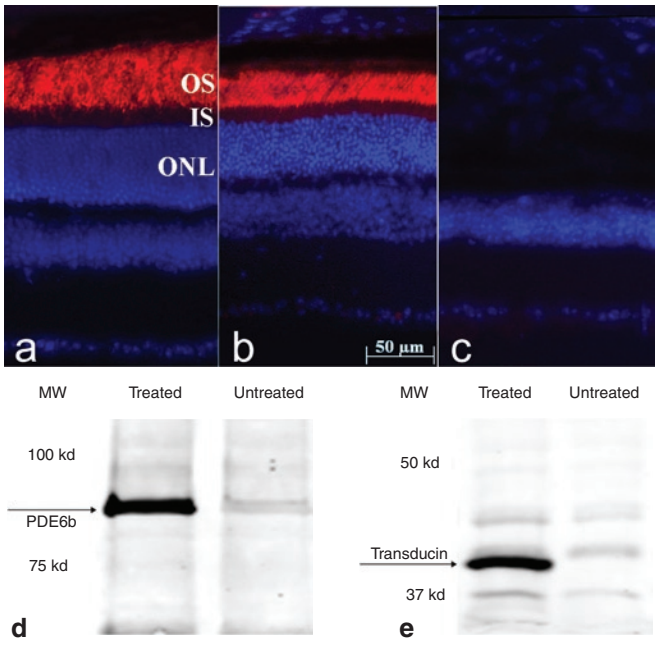

Figure 5 PDEβ expression in treated and untreated eyes of *rd10* mice. PDEβ immunostaining (red) in a 6.5-month old (**a**) uninjected normal C57BL/6J eye, (**b**) treated, and (**c**) untreated eye from one *rd10* mouse. Nuclei were stained with DAPI (blue). Note the robust staining of PDEβ in outer segments of the treated *rd10* eye compared to its absence in untreated, contralateral control eye. Western blot showing (**d**) abundant PDEβ and (**e**) rod transducin-α expression in treated but not in untreated *rd10* eyes. PDEβ, β subunit of rod cGMP-phosphodiesterase; OS, outer segments; IS, inner segments; ONL, outer nuclear layer.

hematoxylin and eosin staining of AAV8 (Y733F)-smCBA-PDEβ-treated *rd10* retinas and contralateral, untreated controls confirmed our OCT results. Retinal structure was largely maintained in treated *rd10* eyes; the outer nuclear layer (ONL) was about 5–8 nuclei thick compared to the 7–10 layers in uninjected C57BL/6J eyes (data not shown). Only one layer of nuclei remained in the ONL of untreated *rd10* eyes. Using a retina from a representative *rd10* mouse which received >90% retinal detachment postinjection, light microscopy at low-magnification revealed a relatively normal ONL throughout the retina (**Figure 4b**, left). In contrast, it was difficult to visualize the ONL in untreated eye of the same *rd10* mouse (**Figure 4b**, right). Higher-magnification images showed that up to 50% of the normal outer segment length and 70% of normal ONL thickness were maintained in the treated *rd10* retina (**Figure 4c**, left). Meanwhile, there was only one incomplete layer of nuclei in the ONL of the untreated eye from the same *rd10* mouse (**Figure 3c**, right). In addition, the outer plexiform layer and inner nuclear layer were also clearly thinned in untreated *rd10* retina (**Figure 4c**, right) relative to that seen in the partner treated eye (**Figure 4c**, left).

Abundant AAV8 (Y733F)-mediated PDEβ expression detected in retinas of treated *rd10* mice

Six months after treatment, PDEβ expression was assayed by immunohistochemistry of treated and untreated retinal sections from *rd10* mice. As seen in normal C57BL/6J retina (**Figure 5a**), strong PDEβ staining is evident in the outer segments of a representative treated *rd10* retina (**Figure 5a**) while no PDEβ expression was observed in the partner untreated retina (**Figure 5c**) from the same *rd10* mouse. Western blot analysis confirmed the presence of the ~90 kDa PDEβ protein in the treated *rd10* retina only (**Figure 5d**). In addition, expression of another phototransduction protein, rod transducin α was also measured by immunoblot and served as another biochemical indicator of photoreceptor cell survival. Our results show that rod transducin α was maintained in treated *rd10* eyes, but not in untreated, contralateral controls in which photoreceptor degeneration is virtually complete (**Figure 5e**).

AAV8 (Y733F)-mediated PDEβ expression prevents secondary neuronal remodeling in the *rd10* retina

Immunocytochemistry confirmed retention of bipolar, horizontal, amacrine, and cone cell morphology in treated *rd10* retinas at 6 months after treatment (**Figure 6**). Cone opsin staining revealed maintenance of well organized cone outer segments in treated eyes whereas its expression was restricted to the cell bodies of aberrant cones in untreated controls (**Figure 6**, left column). As in wild-type controls, photoreceptor synapses in treated *rd10* retinas were abundant (**Figure 6**, middle column). In contrast to untreated eyes, dendrites of rod bipolar cells were well-elaborated and penetrated the cavity of rod spherules in treated retinas (**Figure 7**, right column). Horizontal cell processes were observed in close proximity to the synaptic terminal of rods and cones (**Figure 7**, left column). In contralateral, untreated retinas, second order neurons remodeled upon photoreceptor degeneration, undergoing dendritic atrophy (**Figures 6** and **7**). Lamination of AAV8 (Y733F)-treated *rd10* retinas was preserved and all synaptic markers produced a normal pattern of staining.

DISCUSSION

This study is the first demonstration that long-term restoration of vision and preservation of retinal structure can be achieved in the *rd10* mouse with gene therapy. In addition, it is the first example of AAV8 tyrosine-capsid mutant-mediated therapy in an animal model of disease. Notably, AAV8 (Y733F)-mediated PDEβ expression conferred more effective, long-term therapy to the *rd10* mouse than that seen with standard AAV8 and AAV5 vectors.[25] Previous studies have shown that animal models exhibiting rapid retinal disease onset are refractory to AAV5-, but responsive to AAV8-mediated treatment, both photoreceptor-preferential AAV serotypes.[28] Investigators hypothesized that the onset of transgene expression mediated by AAV5, which is known to be slower relative to AAV8,[30] was not sufficient to provide therapy in an animal model which exhibits very early pathology. Here we show that standard AAV8 was also unable to provide long-term therapy to the *rd10* mouse. Arresting disease pathology in this RP mouse model requires very rapid onset of therapeutic PDEβ expression that is achievable only with the fast-acting AAV8 (Y733F) capsid mutant. Our ERG results (**Figure 3**) highlight the relative abilities of each P14-delivered serotype to restore retinal function to the *rd10* mouse. At 8 weeks after treatment, retinal function was lost in AAV5-treated mice whereas both rod and cone-mediated function were still easily detectable in AAV8-treated mice. However, AAV8-treated rod responses at this time point were already decreasing relative to that seen at 4 weeks after treatment,

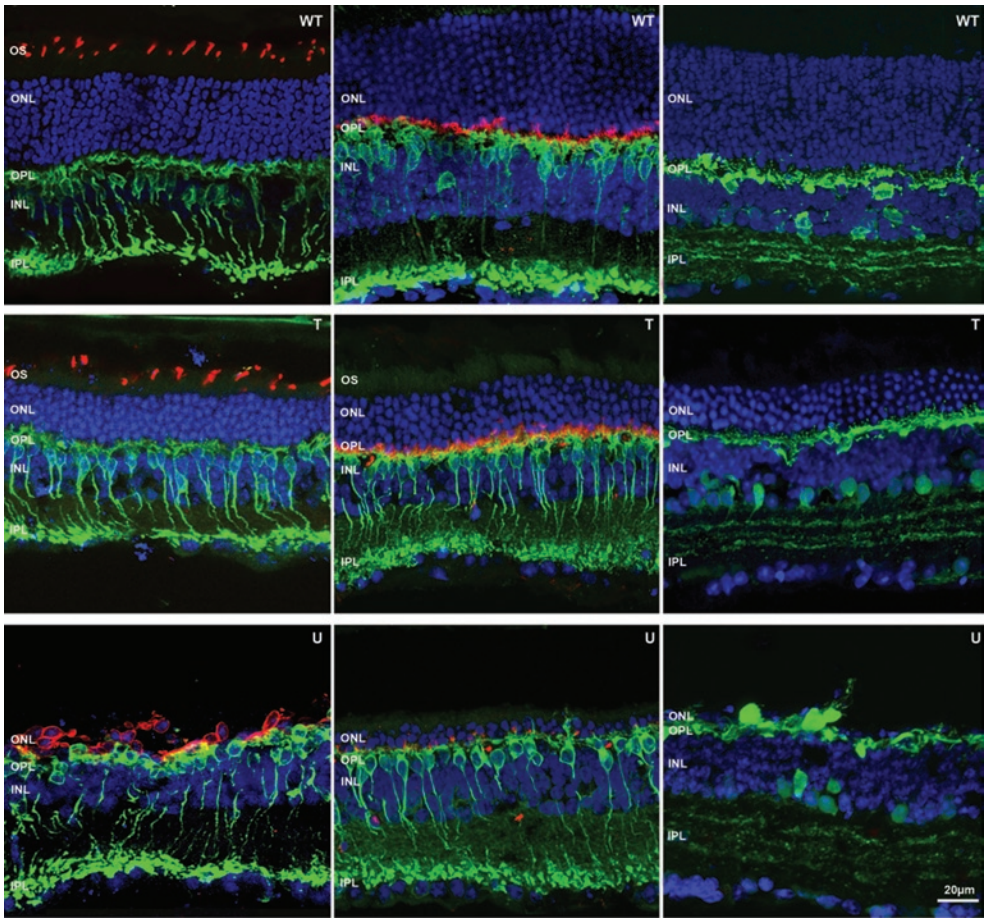

Figure 6 Comparisons of retinal morphology in normal (WT), P14 + 6M treated (T) and untreated (U) *rd10* retinas. Blue: nuclear counterstaining with TOTO-3. Left column, green: rod bipolar cell specific Protein kinase C α (PKC α) Ab staining; red: S- and M-cone opsins Ab staining. Middle, green: bipolar cell specific PKC α Ab staining; red: postsynaptic density protein 95 (PSD95) that stains PR synaptic terminals in the outer plexiform layer (OPL). Right, green: horizontal and amacrine cell specific Calbindin Ab staining. PR, photoreceptor; OS, outer segments; ONL, outer nuclear layer; INL, inner nuclear layer, IPL, inner pexiform layer, WT; wild type.

a result attributable to the pervasive rod degeneration that is typical of this model. Cone responses in AAV8-treated mice were still relatively robust at 8 weeks after treatment, likely because cones had not yet degenerated. In fact, cone responses in AAV8-treated animals increased between 4 and 8 weeks after treatment, a result likely due to the fact that the retina had not fully recovered from the surgical effects of subretinal injection at 4 weeks after treatment. Importantly, rod and cone-mediated retinal function were preserved for at least 6 months in AAV8 (Y733F)-treated mice. Similar to that seen with AAV8, rod and cone responses in AAV8 (Y733F)-treated mice increased between 4 and 8 weeks after treatment, further supporting the notion that mice have not fully recovered from subretinal surgery at 4 weeks after treatment. The slight reductions in rod/cone b-wave amplitudes seen between 8 weeks and 6 months after treatment are attributable to normal age-related decrements in ERG response.[35] We conclude that AAV8 (Y733F) provided more effective therapy in the *rd10* mouse than unmodified vectors because of its increased transduction kinetics relative to standard AAV.[31] Onset of AAV8 (Y733F)-mediated therapeutic PDEβ expression occurred sufficiently early to intervene in the photoreceptor cell death process and prevent inner retinal remodeling. This result highlights the need for careful consideration of vector serotype in any therapeutic platform and supports the use of tyrosine-capsid mutant AAV vectors for the treatment of other diseases which exhibit early pathology and rapid disease progression.

This is the first example, to our knowledge, of using SD-OCT to evaluate a therapeutic end point in a rodent model of retinal disease. The ability to compare relative retinal thicknesses non-invasively in treated versus untreated eyes of *rd10* mice provided us with a valuable tool in which to score therapeutic success. The ability to track a therapeutic outcome (retinal thickness) over time without killing animals greatly enhances the ability to carry out long-term rescue studies (in the *rd10* model as well as others) by dramatically decreasing the number of animals required in the study.

We previously reported that a standard AAV5 vector was capable of delivering functional PDEβ and restoring photoreceptor function, albeit transiently, in *rd10* mice.[25] Animals used in that study were reared in the dark to facilitate therapeutic experiments by slowing retinal degeneration.[25] Therefore, in order to fairly compare the two studies, animals receiving injections of our current vector, AAV8 (Y733F)-smCBA-PDEβ were also dark-reared. One might suggest that the relevance of this study

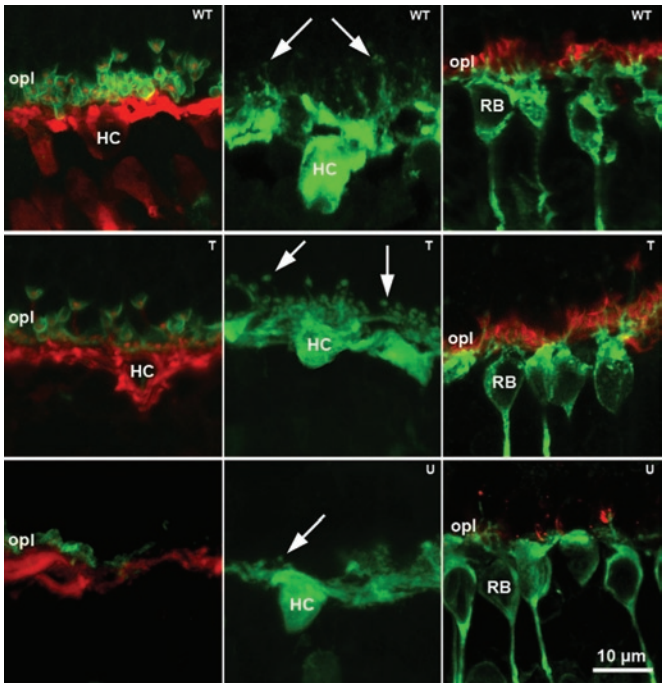

Figure 7 Structural integrity of second order neurons and synaptic contacts in treated retinas. Left column, green: PSD95 that stains PR synaptic terminals in the outer plexiform layer (OPL); red: Calbindin staining of horizontal cells; in treated *rd10* retinas, connections between horizontal cells and photoreceptor are still visible. Red puncta, corresponding to fine dendritic tips of horizontal cells (HC), are observed while penetrating the synaptic cavity of photoreceptor terminals. Middle column, green: Calbindin staining of horizontal cells highlights the preservation of complexity of the dendrites and axonal arborizations of these neurons (arrows) in treated *rd10* retina (middle), compared to the regressed arborizations (arrow) of the untreated *rd10* retina (bottom). Right column, green: rod bipolar cells (RB) specific PKC staining; red: PR synaptic terminals specific PSD95 Ab staining. PSD95 labeling of photoreceptor synaptic terminals in the OPL is still clearly visible in treated *rd10* retina (middle). Rod bipolar cells also show a rich complement of dendrites intermingled with PR terminal (middle) compared to regressed dendrites and scant PR endings observed in the untreated *rd10* counterparts (bottom). T, treated; U; untreated, WT; wild type.

is undermined by the inability to reconstitute such a low light-environment in RP patients. To address this point, we performed the identical experiment on *rd10* mice that were bred, born, and reared in normal, cyclic (12 hour light/12 hour dark) light conditions. Results of this experiment were similar to that seen in the dark-reared, treated *rd10* mice (**Supplementary Figure S1**), which further highlights the improved transduction kinetics of this tyrosine-capsid mutant relative to standard vector. In addition, it suggests that these data are applicable to a physiologically relevant scenario of light conditions typically experienced by RP patients.

RP patients develop night blindness in early adolescence, lose peripheral visual field in young adulthood and eventually retain only a residual central island of vision.[34,36] Like that seen in the *rd10* mouse,[10] rapid photoreceptor degeneration is further complicated by morphological changes in the inner retina.[12] Here we show that P14-delivery of AAV8 (Y733F)-PDEβ was capable of preventing inner retinal remodeling in treated *rd10* eyes. This result has implications for treatment potential in RP patients. The preservation of inner retina allows the opportunity to test alternative restoration strategies after photoreceptor degeneration is complete. For instance, this therapy could be useful for treating older RP patients who haven't undergone complete secondary remodeling. Preservation of inner retinal cells provides a target to which other therapeutic, light sensing proteins, such as channel rhodopsins[37] may be targeted thereby restoring light sensitivity to these patients. It remains to be seen whether delayed treatment in the *rd10* mouse would reverse some aspects of inner retinal remodeling. In addition, a recent study demonstrates the feasibility using embryonic-stage donor cells to replace photoreceptors in the adult retina.[38] It is likely that the success of photoreceptor cell transplantation will depend on the ability of these transplanted photoreceptors to make appropriate synaptic contacts with inner retinal neurons, a result which will likely only be achieved in a retina which hasn't undergone extensive inner retinal remodeling. Therefore, the ability to preserve inner retinal remodeling in the *rd10* mouse could have implications in late stage RP patients who may be better candidates for stem cell therapy as opposed to photoreceptor-targeted gene-replacement therapy.

Using a fast-acting tyrosine-capsid mutant AAV8 (Y733F) vector, we have shown for the first time that gene therapy effectively restores long-term vision to an animal model of PDEβ-based RP. In addition, this study supports the use of AAV8 (Y733F), and perhaps other tyrosine-capsid mutants for the treatment of other rapidly degenerating models of retinal disease. Our results suggest that AAV-based gene-replacement therapy for human RP is now a viable therapeutic option.

MATERIALS AND METHODS

Animals. C57 BL/6J mice and the congenic inbred strain of *rd10* mice were obtained from the Jackson Laboratory (Bar Harbor, ME) and bred at the University of Florida. About 100 mice were used in this study. All mice were maintained in the University of Florida Health Science Center Animal Care Service Facilities in a dark environment until postnatal day 28 when they were transferred to a 12 hour /12 hour light/dark cycle with <15 ft-c environmental illumination. Four *rd10* mice were raised in normal 12 hour /12 hour light/dark cycle with <15 ft-c environmental illumination before and after the treatment. All experiments were approved by the Institutional Animal Care and Use Committee in University of Florida and conducted in accordance with the ARVO Statement for the Use of Animals in Ophthalmic and Vision Research and National Institutes of Health regulations.

Construction of AAV vectors. AAV serotype 8 capsids containing a point mutation in surface-exposed tyrosine residues, AAV8 (Y733F) exhibit higher transduction efficiency in photoreceptors and a faster onset of expression than other AAV serotypes when delivered to the subretinal space[33] and were therefore used for packaging the current vector. For purposes of ERG comparison, the vector was also packaged in standard serotype 8 (AAV8) and serotype 5 (AAV5) capsids. Vector plasmids were constructed as previously described.[33] Wild-type murine Pde6b complementary DNA was placed under the control of the ubiquitous, constitutive smCBA promoter[25,39] to generate pTR-smCBA-PDEβ. AAV vectors were packaged and purified according to previously reported methods.[40]

Subretinal injections. Litters of *rd10* mice were kept in a dark environment (<5 lux) until P14 when 1 µl of AAV8 (Y733F)-smCBA-PDEβ (10^{10} vector genomes) was subretinally injected into one eye. Subsets of

mice were also injected in one eye only with equal volumes and concentrations of either AAV5-smCBA-PDEβ or AAV8-smCBA-PDEβ. The other eye remained uninjected. The animals were then maintained for 2 more weeks in the same dark environment before moving them into a normal 12 hour/12 hour vivarium cycling room light. Subretinal injections were performed with previously described method.[25] In animals with no apparent surgical complications, only those whose initial retinal blebs occupied >80% of the retina were retained for further evaluation. Twenty *rd10* mice met this criterion, which resulted in at least three animals for each experiment. Following all injections, 1% atropine eye drops and neomycin/polymyxin B/dexamethasone ophthalmic ointments were given.

Optomotor testing. Photopic and scotopic visual acuities and contrast sensitivities of AAV8 (Y733F)-smCBA-PDEβ-treated and untreated rd10 eyes were measured using a two-alternative forced choice paradigm as described previously with minor modifications.[41,42] Thresholds for each eye were determined simultaneously via stepwise functions for correct responses in both the clockwise and counter-clockwise direction. Acuity was defined as the highest spatial frequency (100% contrast) yielding a threshold response, and contrast sensitivity was defined as 100 divided by the lowest percent contrast (at a fixed frequency examined) yielding a threshold response. For both photopic and scotopic acuity, the initial stimulus was a 0.200 cyc/deg sinusoidal pattern with a fixed 100% contrast. For photopic contrast sensitivity measurements, the initial pattern was presented at 100% contrast, with a fixed spatial frequency of 0.128 cyc/deg. For scotopic contrast sensitivity measurements, the spatial frequency was fixed at 0.031 cyc/deg, a spatial frequency tuned for rod vision.[43] All patterns were presented at a speed of 12 degrees per second. Photopic vision was measured at a mean luminance of 70 cd/m^2. For scotopic measurements, mice were dark-adapted overnight and light levels were attenuated to 3.5×10^{-5} cd/m^2 through the use of neutral density filters. Visual acuities and contrast sensitivities were measured for both eyes of each mouse four to six times over a period of 1–2 weeks. Wild-type control animals were 7 months old at testing time ($n = 4$), and P14 treated rd10 mice were 6.5 months old ($n = 4$). Unpaired *t*-tests were carried out on acuity and percent contrast values to determine significance of results.

Electroretinography. At 4 weeks, 8 weeks and 6 months following subretinal injection, a UTAS Visual Diagnostic System with a Big Shot Ganzfeld (LKC Technologies, Gaithersburg, MD) was used for ERG recording with the same methods we previously described[42] with minor modifications. Dark-adapted-ERGs were recorded at 0.4 log cd-s/m^2 intensity and the interstimulus interval was 30 seconds; 10 signals were averaged for conventional dark-adapted ERG. Fifty signals were averaged for photopic measurements taken at 1.4 log cd-s/m^2 in the presence of 30 cd/m^2 background light (the interstimulus interval was 0.4 seconds) using LKC software, EM for Windows version 7.0 (LKC Technologies). Ganzfeld illumination with white light was applied for duration of 2.4 ms. B-wave amplitudes were defined as the difference between the trough and peak of each waveform. Scotopic and photopic b-wave maximum amplitudes from different treated rd10 eyes were averaged and used to generate SEs. ERG data are presented as mean ± SD. Statistical significance was determined with paired *t*-test. Significance was defined as a *P* value of less than 0.05.

SD-OCT and histology. Six months post-treatment, pupils of both AAV8 (Y733F)-smCBA-PDEβ-treated and untreated rd10 eyes were dilated with 1% atropine and 2.5% phenylephrine hydrochloride. Mice were then anesthetized as previously described.[42] One drop of 2.5% hydroxypropyl methylcellulose was administrated to eyes before examination. SD-OCT was performed noninvasively using a machine manufactured by Bioptigen (Durham, NC). Three lateral images (nasal to temporal) were collected, starting 3 mm above the meridian crossing through the center of the ON, at the ON meridian and 3 mm below ON meridian. A corresponding box centered on the ON with eight measurement points separated by 3 mm from each other was created. Corresponding neural retina thickness for treated and untreated rd10 eyes was compared at each point by measuring the distance from the vitreal face of the ganglion cell layer to the apical face of the retinal pigment epithelium. Statistical significance was determined by a paired *t*-test with *P* values of <0.05 considered significant.

Following SD-OCT examination, both treated and untreated *rd10* eyes were enucleated and eyecups prepared for light microscopic examination. Structural evaluation of the treated and untreated eyes was done as previously described with some modifications.[44] Briefly eyes were fixed in 4% paraformaldehyde solution and embedded in paraffin. Sections (4 μm) were stained with hematoxylin and eosin before photographing with a Zeiss CD25 microscope (Axiovision Carl Zeiss MicroImaging, Thornwood, NY) fitted with Axiovision Rel. 4.6 software.

Immunocytochemistry for PDEβ expression. Eyes from AAV8 (Y733F)-smCBA-PDEβ-treated and untreated rd10 mice, along with age-matched C57BL/6J mice, were enucleated and the eyecups were processed as described previously.[45] Retinal sections were prepared for PDEβ antibody staining according to previously described methods.[25]

Western blot analysis. AAV8(Y733F)-smCBA-PDEβ-treated and untreated rd10 eyes were carefully dissected, and the PDEβ protein was detected by western blotting as previously described.[25] Briefly, the eyecups were homogenized by sonication in a buffer containing 0.23 mol sucrose, 2 mmol/l EDTA, 5 mmol/l Tris–HCl (pH 7.5), and 0.1 mmol/l phenylmethylsulfonyl fluoride. After centrifugation, aliquot extracts containing equal amounts of protein (30 μg) were electrophoresed, transferred, and probed either with a primary antibody against PDEβ (rabbit polyclonal PA1-722; Thermo Scientific Life Science Research Products, Rockford, IL) or polyclonal antibody against rod transducin α (sc-389, Santa Cruz Biotechnology, Santa Cruz, CA). Visualization of specific bands was performed using the Odyssey Infrared Fluorescence Imaging System (Odyssey; Li-Cor, Lincoln, NE).

Immunocytochemistry for inner retinal neurons and their connections in rd10 mice. Morphology of retinal cells and the integrity of their synaptic connections in AAV8 (Y733F)-smCBA-PDEβ-treated, untreated, and wild-type controls were assessed by immunocytochemistry with cell type-specific antibodies as previously reported.[10] Briefly, following antibody staining slides were examined by high resolution confocal microscopy, using a Leica TCS SP confocal microscope (Leica, Heidelberg, Germany). For cone identification, antibodies against S- and M-cone opsin were used. Photoreceptor synaptic terminals in the outer plexiform layer were labeled with PSD95. Protein kinase C–α was used to label rod bipolar cells and calbindin was used to label horizontal and amacrine cells. Sections were counterstained with the fluorescent nuclear marker TOTO-3. Images were obtained using ×40 and ×63 high numerical aperture objectives. Sections from AAV8 (Y733F)-smCBA-PDEβ-treated and untreated control eyes at similar eccentricities were compared.

SUPPLEMENTARY MATERIAL

Figure S1. Scotopic and photopic ERGs from treated and untreated eyes of a representative *rd10* mouse raised in normal light cycle.

ACKNOWLEDGMENTS

We thank Vince Chiodo, Thomas Doyle (vector production) and Issam McDoom (SD-OCT) at the University of Florida for their technical support. We also acknowledge NIH grants EY018331, EY13729, EY11123, NS36302, EY08571, EY19943, EY014046, EY06360, EY017246 (D.E.), EY00067 (R.B.) and grants from the Macular Vision Research Foundation, Foundation Fighting Blindness, Fight for Sight (D.E.), Lions of Central NY, NASA (R.B.), Juvenile Diabetes Research Foundation and Research to Prevent Blindness, Inc. for partial support of this work. W.W.H. and the University of Florida have a financial interest in the use of AAV therapies, and own equity in a company (AGTC) that might, in the future, commercialize some aspects of this work.

REFERENCES

1. McLaughlin, ME, Ehrhart, TL, Berson, EL and Dryja, TP (1995). Mutation spectrum of the gene encoding the β subunit of rod phosphodiesterase among patients with autosomal recessive retinitis pigmentosa. *Proc Natl Acad Sci USA* **92**: 3249–3253.
2. Danciger, M, Blaney, J, Gao, YQ, Zhao, DY, Heckenlively, JR, Jacobson, SG *et al.* (1995). Mutations in the PDE6B gene in autosomal recessive retinitis pigmentosa. *Genomics* **30**: 1–7.
3. McLaughlin, ME, Sandberg, MA, Berson, EL and Dryja, TP (1993). Recessive mutations in the gene encoding the β -subunit of rod phosphodiesterase in patients with retinitis pigmentosa. *Nat Genet* **4**: 130–134.
4. Bennett, J, Tanabe, T, Sun, D, Zeng, Y, Kjeldbye, H, Gouras, P *et al.* (1996). Photoreceptor cell rescue in retinal degeneration (rd) mice by *in vivo* gene therapy. *Nat Med* **2**: 649–654.
5. Jomary, C, Vincent, KA, Grist, J, Neal, MJ and Jones, SE (1997). Rescue of photoreceptor function by AAV-mediated gene transfer in a mouse model of inherited retinal degeneration. *Gene Ther* **4**: 683–690.
6. Takahashi, M, Miyoshi, H, Verma, IM and Gage, FH (1999). Rescue from photoreceptor degeneration in the rd mouse by human immunodeficiency virus vector-mediated gene transfer. *J Virol* **73**: 7812–7816.
7. Chang, B, Hawes, NL, Hurd, RE, Davisson, MT, Nusinowitz, S and Heckenlively, JR (2002). Retinal degeneration mutants in the mouse. *Vision Res* **42**: 517–525.
8. Chang, B, Hawes, NL, Pardue, MT, German, AM, Hurd, RE, Davisson, MT *et al.* (2007). Two mouse retinal degenerations caused by missense mutations in the β -subunit of rod cGMP phosphodiesterase gene. *Vision Res* **47**: 624–633.
9. Gargini, C, Terzibasi, E, Mazzoni, F and Strettoi, E (2007). Retinal organization in the retinal degeneration 10 (rd10) mutant mouse: a morphological and ERG study. *J Comp Neurol* **500**: 222–238.
10. Strettoi, E, Porciatti, V, Falsini, B, Pignatelli, V and Rossi, C (2002). Morphological and functional abnormalities in the inner retina of the rd/rd mouse. *J Neurosci* **22**: 5492–5504.
11. Strettoi, E, Pignatelli, V, Rossi, C, Porciatti, V and Falsini, B (2003). Remodeling of second-order neurons in the retina of rd/rd mutant mice. *Vision Res* **43**: 867–877.
12. Jacobson, SG, Sumaroka, A, Aleman, TS, Cideciyan, AV, Danciger, M and Farber, DB (2007). Evidence for retinal remodelling in retinitis pigmentosa caused by PDE6B mutation. *Br J Ophthalmol* **91**: 699–701.
13. Banin, E, Cideciyan, AV, Alemán, TS, Petters, RM, Wong, F, Milam, AH *et al.* (1999). Retinal rod photoreceptor-specific gene mutation perturbs cone pathway development. *Neuron* **23**: 549–557.
14. Jones, BW, Watt, CB, Frederick, JM, Baehr, W, Chen, CK, Levine, EM *et al.* (2003). Retinal remodeling triggered by photoreceptor degenerations. *J Comp Neurol* **464**: 1–16.
15. Marc, RE, Jones, BW, Watt, CB, Vazquez-Chona, F, Vaughan, DK and Organisciak, DT (2008). Extreme retinal remodeling triggered by light damage: implications for age related macular degeneration. *Mol Vis* **14**: 782–806.
16. Milam, AH, Li, ZY and Fariss, RN (1998). Histopathology of the human retina in retinitis pigmentosa. *Prog Retin Eye Res* **17**: 175–205.
17. Milam, AH, Barakat, MR, Gupta, N, Rose, L, Aleman, TS, Pianta, MJ *et al.* (2003). Clinicopathologic effects of mutant GUCY2D in Leber congenital amaurosis. *Ophthalmology* **110**: 549–558.
18. Pignatelli, V, Cepko, CL and Strettoi, E (2004). Inner retinal abnormalities in a mouse model of Leber's congenital amaurosis. *J Comp Neurol* **469**: 351–359.
19. Puthussery, T and Taylor, WR (2010). Functional changes in inner retinal neurons in animal models of photoreceptor degeneration. *Adv Exp Med Biol* **664**: 525–532.
20. Varela, C, Igartua, I, De la Rosa, EJ and De la Villa, P (2003). Functional modifications in rod bipolar cells in a mouse model of retinitis pigmentosa. *Vision Res* **43**: 879–885.
21. Strettoi, E and Pignatelli, V (2000). Modifications of retinal neurons in a mouse model of retinitis pigmentosa. *Proc Natl Acad Sci USA* **97**: 11020–11025.
22. Margolis, DJ, Newkirk, G, Euler, T and Detwiler, PB (2008). Functional stability of retinal ganglion cells after degeneration-induced changes in synaptic input. *J Neurosci* **28**: 6526–6536.
23. Mazzoni, F, Novelli, E and Strettoi, E (2008). Retinal ganglion cells survive and maintain normal dendritic morphology in a mouse model of inherited photoreceptor degeneration. *J Neurosci* **28**: 14282–14292.
24. Stasheff, SF (2008). Emergence of sustained spontaneous hyperactivity and temporary preservation of OFF responses in ganglion cells of the retinal degeneration (rd1) mouse. *J Neurophysiol* **99**: 1408–1421.
25. Pang, JJ, Boye, SL, Kumar, A, Dinculescu, A, Deng, W, Li, J *et al.* (2008). AAV-mediated gene therapy for retinal degeneration in the rd10 mouse containing a recessive PDEβ mutation. *Invest Ophthalmol Vis Sci* **49**: 4278–4283.
26. Boatright, JH, Moring, AG, McElroy, C, Phillips, MJ, Do, VT, Chang, B *et al.* (2006). Tool from ancient pharmacopoeia prevents vision loss. *Mol Vis* **12**: 1706–1714.
27. Otani, A, Dorrell, MI, Kinder, K, Moreno, SK, Nusinowitz, S, Banin, E *et al.* (2004). Rescue of retinal degeneration by intravitreally injected adult bone marrow-derived lineage-negative hematopoietic stem cells. *J Clin Invest* **114**: 765–774.
28. Sun, X, Pawlyk, B, Xu, X, Liu, X, Bulgakov, OV, Adamian, M *et al.* (2010). Gene therapy with a promoter targeting both rods and cones rescues retinal degeneration caused by AIPL1 mutations. *Gene Ther* **17**: 117–131.
29. Pawlyk, BS, Smith, AJ, Buch, PK, Adamian, M, Hong, DH, Sandberg, MA *et al.* (2005). Gene replacement therapy rescues photoreceptor degeneration in a murine model of Leber congenital amaurosis lacking RPGRIP. *Invest Ophthalmol Vis Sci* **46**: 3039–3045.
30. Natkunarajah, M, Trittibach, P, McIntosh, J, Duran, Y, Barker, SE, Smith, AJ *et al.* (2008). Assessment of ocular transduction using single-stranded and self-complementary recombinant adeno-associated virus serotype 2/8. *Gene Ther* **15**: 463–467.
31. Zhong, L, Zhao, W, Wu, J, Li, B, Zolotukhin, S, Govindasamy, L *et al.* (2007). A dual role of EGFR protein tyrosine kinase signaling in ubiquitination of AAV2 capsids and viral second-strand DNA synthesis. *Mol Ther* **15**: 1323–1330.
32. Zhong, L, Li, B, Mah, CS, Govindasamy, L, Agbandje-McKenna, M, Cooper, M *et al.* (2008). Next generation of adeno-associated virus 2 vectors: point mutations in tyrosines lead to high-efficiency transduction at lower doses. *Proc Natl Acad Sci USA* **105**: 7827–7832.
33. Petrs-Silva, H, Dinculescu, A, Li, Q, Min, SH, Chiodo, V, Pang, JJ *et al.* (2009). High-efficiency transduction of the mouse retina by tyrosine-mutant AAV serotype vectors. *Mol Ther* **17**: 463–471.
34. Gabriele, ML, Ishikawa, H, Schuman, JS, Bilonick, RA, Kim, JS, Kagemann, L *et al.* (2010). Reproducibility of Spectral-Domain Optical Coherence Tomography Total Retinal Thickness Measurements in Mice. *Invest Ophthalmol Vis Sci* (epub ahead of print).
35. Li, C, Cheng, M, Yang, H, Peachey, NS and Naash, MI (2001). Age-related changes in the mouse outer retina. *Optom Vis Sci* **78**: 425–430.
36. Berson, EL (2007). Long-term visual prognoses in patients with retinitis pigmentosa: the Ludwig von Sallmann lecture. *Exp Eye Res* **85**: 7–14.
37. Bi, A, Cui, J, Ma, YP, Olshevskaya, E, Pu, M, Dizhoor, AM *et al.* (2006). Ectopic expression of a microbial-type rhodopsin restores visual responses in mice with photoreceptor degeneration. *Neuron* **50**: 23–33.
38. Lakowski, J, Baron, M, Bainbridge, J, Barber, AC, Pearson, RA, Ali, RR *et al.* (2010). Cone and rod photoreceptor transplantation in models of the childhood retinopathy Leber congenital amaurosis using flow-sorted Crx-positive donor cells. *Hum Mol Genet* **19**: 4545–4559.
39. Haire, SE, Pang, J, Boye, SL, Sokal, I, Craft, CM, Palczewski, K *et al.* (2006). Light-driven cone arrestin translocation in cones of postnatal guanylate cyclase-1 knockout mouse retina treated with AAV-GC1. *Invest Ophthalmol Vis Sci* **47**: 3745–3753.
40. Hauswirth, WW, Lewin, AS, Zolotukhin, S and Muzyczka, N (2000). Production and purification of recombinant adeno-associated virus. *Meth Enzymol* **316**: 743–761.
41. Boye, SE, Boye, SL, Pang, J, Ryals, R, Everhart, D, Umino, Y *et al.* (2010). Functional and behavioral restoration of vision by gene therapy in the guanylate cyclase-1 (GC1) knockout mouse. *PLoS ONE* **5**: e11306.
42. Pang, J, Boye, SE, Lei, B, Boye, SL, Everhart, D, Ryals, R *et al.* (2010). Self-complementary AAV-mediated gene therapy restores cone function and prevents cone degeneration in two models of Rpe65 deficiency. *Gene Ther* **17**: 815–826.
43. Umino, Y, Solessio, E and Barlow, RB (2008). Speed, spatial, and temporal tuning of rod and cone vision in mouse. *J Neurosci* **28**: 189–198.
44. Pang, J, Cheng, M, Stevenson, D, Trousdale, MD, Dorey, CK and Blanks, JC (2004). Adenoviral-mediated gene transfer to retinal explants during development and degeneration. *Exp Eye Res* **79**: 189–201.
45. Pang, JJ, Chang, B, Hawes, NL, Hurd, RE, Davisson, MT, Li, J *et al.* (2005). Retinal degeneration 12 (rd12): a new, spontaneously arising mouse model for human Leber congenital amaurosis (LCA). *Mol Vis* **11**: 152–162.